

- [26] L. K. Steinrauf, J. A. Hamilton, B. C. Braden, J. R. Murrel, M. D. Benson, *J. Biol. Chem.* **1993**, 268, 2425.  
 [27] G. R. Desiraju, *Crystal Engineering: The Design of Organic Solids*, Elsevier, Amsterdam, **1989**.  
 [28] J.-M. Lehn, *Supramolecular Chemistry: Concepts and Perspectives*, VCH, Weinheim, **1995**.

## Spin-Density Map of the Triplet Ground State of a Titanium(IV) Complex with Schiff-Base Diquinone Radical Ligands: An Investigation Using Polarized-Neutron Diffraction and Density-Functional Theory\*\*

Yves Pontillon, Alessandro Bencini, Andrea Caneschi, Andrea Dei, Dante Gatteschi,\* Béatrice Gillon,\* Claudio Sangregorio, John Stride, and Federico Totti

During the last decade, the design of new molecular ferromagnets has been a field of growing interest.<sup>[1]</sup> Ferromagnetic interactions between organic radicals, although rare, are now recognized as real.<sup>[2–5]</sup> The final goal of obtaining molecular-based ferromagnets may be achieved if, for example, the individual building blocks carrying unpaired electrons are arranged such that the magnetic orbitals remain orthogonal to each other.<sup>[6]</sup> With this in mind, attempts have been made to use organic radicals bound to diamagnetic metal ions and some elegant examples of moderate ferromagnetic coupling have been reported.<sup>[7]</sup> In particular, a titanium(IV) complex  $\text{TiL}_2$ , where L is the dianion of the radical ligand 3,5-di-*tert*-butyl-1,2-semiquinonato-1-(2-hydroxy-3,5-di-*tert*-butyl-phenyl)imine, has been found to be characterized by a triplet ground state arising from a ferromagnetic interaction ( $J = 56 \text{ cm}^{-1}$ ) between the two  $\frac{1}{2}$ -spin coordinated radical ligands.<sup>[8]</sup> This compound crystallizes in the triclinic  $P\bar{1}$  space group. The metal ion is octahedrally coordinated by the two ligands, which occupy the meridional sites of the coordination polyhedron (Figure 1). The two ligands are orthogonal to each

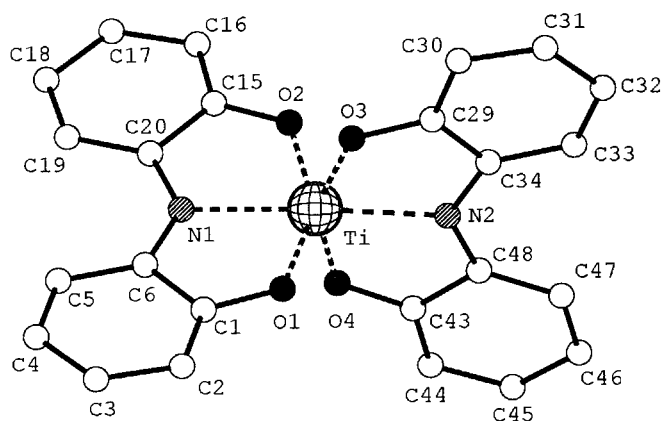


Figure 1. View of the  $\text{TiL}_2$  molecule showing the numbering of the atoms. The *tert*-butyl groups are omitted for clarity.

other and the dihedral angles between the aromatic rings in the two ligands are  $9.7^\circ$  and  $5.4^\circ$ , respectively.

It has been proposed<sup>[8]</sup> that the triplet ground state is stabilized by the topological degeneracy of the two magnetic orbitals of the ligands. Assuming an overall  $C_{2v}$  symmetry for the complex, the two  $\pi^*$  magnetic orbitals span the  $b_1$  and  $b_2$  irreducible representations and are, therefore, orthogonal to each other and this provides a rationalization of the observed ferromagnetic coupling.

The exchange interactions between the two radicals may arise from both direct overlap between the ligand magnetic orbitals (the shortest interligand oxygen–oxygen distances are about  $2.7 \text{ \AA}$ ) and superexchange as mediated by metal orbitals.<sup>[8, 9]</sup> In the former case, the unpaired spin density (SD) is expected to be located onto the ligands, whereas in the latter a sizeable SD must be observed also on the metal ion, which, according to the formal  $\text{Ti}^{4+}$  charge, has a  $d^0$  configuration.

In this communication, we report the preliminary results concerning a polarized neutron diffraction (PND) study of the  $\text{TiL}_2$  compound. The PND technique is well adapted for measuring the spin-density distribution in magnetic crystalline molecular compounds.<sup>[10, 11]</sup> It is applicable to single crystals in which the spin density has been partly or totally aligned by an external magnetic field.

The PND experiment was performed on the polarized-neutron lifting-counter diffractometer 5c1 at the Orphee reactor (CEA-Saclay, France). A small  $\text{TiL}_2$  crystal,  $2 \times 2 \times 1 \text{ mm}^3$ , was mounted with the  $a$  axis parallel to the  $7 \text{ T}$  applied magnetic field. The flipping ratios ( $F_N$ ) of the more intense reflections were measured:  $F_N = 39:1$  at  $T = 1.5 \text{ K}$ . By measuring the integrated nuclear intensities of the same set of reflections in a zero field,<sup>[12]</sup> it was found that the room temperature X-ray crystal structure<sup>[8]</sup> could be used to model and normalize the  $F_N$  and to determine their phase. The magnetic structure factors ( $F_M$ ) were obtained through standard techniques.<sup>[12]</sup>

There are different possible approaches to analyze the PND experimental data.<sup>[11]</sup> A versatile method is based on the modeling of the spin-density distribution  $s(r)$  followed by a direct expansion of the spin density around the nuclei. This

[\*] D. Gatteschi, Y. Pontillon,<sup>[+]</sup> A. Bencini, A. Caneschi, A. Dei, C. Sangregorio, F. Totti, Dipartimento di Chimica Università degli Studi di Firenze Via Maragliano 77, 50144 Florence (Italy) Fax: (+39)055-35-48-45 E-mail: gatteschi@blu.chim1.unifi.it

B. Gillon, J. Stride CEA Saclay Laboratoire Léon Brillouin 91191 Gif-sur-Yvette Cedex (France) Fax: (+33)01-69-08-82-61 E-mail: gillon@bali.saclay.cea.fr

[+] Present address: Institut Laue Langevin 6 rue J. Horowitz BP 156, 38042 Grenoble Cedex 9 (France)

[\*\*] This work was supported by the 3MD EU network (contract ERB 4061 PL 97-0197).

method incorporates a superposition of aspherical densities, expressed at any point  $r$  as atomic contributions developed in series of real spherical harmonics [Eq. (1)], where  $l$  and  $n$  are the principal and magnetic quantum numbers, and  $R_l(r)$  and  $y_{lm}(\theta, \varphi)$  the radial and angular part respectively. Consequently, the spin distribution depends on parameters—the population coefficients  $P_{lm}$  and the Slater-type radial function of the spin density  $R_l(r)$ —which are determined by the best fit of the experimental data.

$$s(r) = \sum_{\text{atoms}} \sum_l R_l(r) \sum_m P_{lm} y_{lm}(\theta, \varphi) \quad (1)$$

For the present case, since the number of the experimental  $F_M$  values are low due to the small size of the crystal, the following constraints were used: 1) the carbon atoms of the *tert*-butyl groups were not taken into account; 2) only spherical contributions were refined; and 3) the refinement was performed in two stages.<sup>[12]</sup> For the refinement, first the carbon atoms of each phenyl ring were successively refined, together with nitrogen, oxygen, and titanium atoms. Only contributions from the C1, C6, C15, C20, C29, C34, C43, C48, N1, N2, and Ti atoms were found to be significant. Consequently, only contributions from these atoms were kept in the second refinement stage<sup>[13]</sup>. Table 1 displays the resulting

Table 1. Atomic spin populations obtained by multipole refinement and standard deviations in parentheses, together with the results of DFT calculations.

Atoms	Experimental <sup>[a]</sup> ( $\mu_B$ )	DFT Calculations ( $\mu_B$ )	
		VWN-Stoll <sup>[b]</sup>	BLYP <sup>[c]</sup>
C1	0.24(4)	0.09	0.10
C6	0.12(6)	0.01	−0.01
C15	0.22(5)	0.11	0.12
C20	0.10(7)	0.01	−0.01
C29	0.24(6)	0.10	0.12
C34	−0.05(4)	0.00	−0.01
C43	0.20(5)	0.10	0.11
C48	0.04(4)	0.01	−0.01
N1	0.21(7)	0.25	0.27
N2	0.19(7)	0.23	0.26
Ti	0.17(3)	0.09	0.08
O1	−0.03(6)	0.06	0.06
O2	0.03(6)	0.07	0.07
O3	0.01(6)	0.06	0.06
O4	0.04(6)	0.07	0.07

[a] Refinement statistics:  $wR(F) = 16.3\%$ ,  $\chi^2 = 1.31$ . [b] Local spin-density approximation. [c] Generalized gradient approximation.

experimental spin populations, together with the statistics of refinement and the oxygen spin populations obtained in the first stage. Figure 2 shows the projection of the spin density onto the mean plane of the two ligands.

The main features of the obtained spin-density distribution are the following: 1) no significant spin population is observed on the oxygen atoms; 2) strong, positive spin populations are found on each carbon atom corresponding to the four C–O bonds of the complex (C1, C15, C29, C43); 3) strong, positive spin populations are obtained on the N1 and N2 atoms with a small asymmetry favoring N1; and 4) a significant degree of the spin density is found on the titanium center.

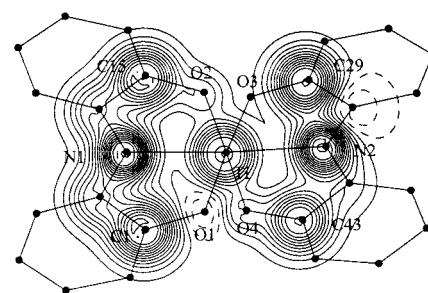


Figure 2. Spin-population density projected onto the mean plane generated by the coordinated ligands L. Contour steps are  $0.008 \mu_B \text{ Å}^{-2}$ ; positive contours (—), negative contours (---).

Although the experimental results are less accurate than those generally obtained from the PND technique (due to the limitation to 39 reflections), the observed effects are significant. The experimental determination of SD in this complex provides primarily clear answers concerning questions of the pathway of ferromagnetic interactions. Titanium(IV) is a  $d^0$  ion, so the spin population observed on that atom is due to a “transfer” from the ligands. Consequently, the metal ion is involved in the exchange pathway. The very low spin density on the oxygen atoms suggests that these atoms do not play any major role in determining interligand magnetic interactions. Therefore, an exchange pathway due to the direct overlap of the ligand magnetic orbitals can be ruled out.

These results are in agreement with the exchange mechanism suggested, on the basis of density functional theory (DFT) calculations, for the exchange coupling constants in the  $\text{TiL}_2$  and  $\text{SnL}_2$  complexes.<sup>[9]</sup> Here, we have applied the same computational model to calculate the spin-density distribution on the  $\text{TiL}_2$  complex. This calculation<sup>[14]</sup> was performed on a model molecule in which the *tert*-butyl groups were replaced by hydrogen atoms based on the room temperature X-ray crystal structure. The same model molecule, under  $C_{2v}$  symmetry, was used in ref. [9]. The spin populations, computed using the Mulliken population analysis,<sup>[15]</sup> calculations were performed using the local spin-density approximation (VWN-Stoll)<sup>[16]</sup> and the generalized gradient approximation (BLYP)<sup>[17]</sup> for the exchange and correlation functionals. The results of the calculations are reported and compared with the experiment (Table 1). In agreement with the experimental results, a larger spin density is computed on the nitrogen atoms than on the oxygen atoms and a sizeable spin density, although smaller than the measured value, is found on the titanium atom. The sources of the spin density are 74% from the Ti 3d and 26% from the 3p orbitals. The values of the computed density are almost independent of the functional used.

A second series of PND experiments, utilizing a larger crystal, is planned in order to increase the precision of the results and to permit a description of the spin density beyond the spherical contributions. The latter point is of utmost importance in order to extract from the results which of the metal orbitals are involved in the exchange mechanism and to determine the geometries of the 2p orbitals in the C1–C6–N1–C20–C15 and C29–C34–N2–C48–C43 fragments.

Received: December 3, 1999 [Z14355]

- [1] *Magnetic Molecular Materials* (Eds.: D. Gatteschi, O. Kahn, J. S. Miller, F. Palacio), Kluwer Academic Publishers, Dordrecht, **1991**.
- [2] A. Caneschi, F. Ferraro, D. Gatteschi, A. Le Lirzin, M. Novak, E. Rentschler, R. Sessoli, *Adv. Mater.* **1995**, *7*, 476.
- [3] M. Kinoshita, P. Turek, H. Tamura, K. Nozana, D. Shiomi, Y. Nakazama, M. Ishikawa, M. Takahashi, K. Awaga, T. Inabe, Y. Muruyama, *Chem. Lett.* **1991**, 1225.
- [4] H. Iwamura, K. Inoue, N. Koga, T. Hayamizu in *Magnetism: A Supramolecular Function* (Ed: O. Kahn), NATO ASI Series C484, Kluwer Academic Publishers, Dordrecht, **1996**, pp. 157–180.
- [5] J. Cirujeda, M. Mas, E. Molins, F. L. de Panthou, J. Laugier, J. G. Park, C. Paulsen, P. Rey, C. Rovira, J. Veciana, *J. Chem. Soc. Chem. Commun.* **1995**, 709.
- [6] a) O. Kahn, J. Larionova, L. Ouahab, *Chem. Commun.* **1999**, 945; b) J. S. Miller, A. J. Epstein, *Chem. Commun.* **1998**, 1319.
- [7] a) A. Cogne, A. Grand, P. Rey, R. Subra, *J. Am. Chem. Soc.* **1989**, *111*, 3230; b) D. M. Adam, A. L. Rheingold, A. Dei, D. N. Hendrickson, *Angew. Chem.* **1993**, *105*, 434; *Angew. Chem. Int. Ed. Engl.* **1993**, *32*, 391; c) H. Oshio, M. Yamamoto, T. Ito, *J. Chem. Soc. Dalton Trans.* **1999**, 2641.
- [8] a) A. Caneschi, A. Dei, D. Gatteschi, *J. Chem. Soc. Chem. Commun.* **1992**, 630; b) S. Bruni, A. Caneschi, F. Cariati, C. Delfs, A. Dei, D. Gatteschi, *J. Am. Chem. Soc.* **1994**, *116*, 1388.
- [9] A. Bencini, I. Ciofini, E. Giannasi, C. A. Daul, K. Doclo, *Inorg. Chem.* **1998**, *37*, 3719.
- [10] a) Y. Pontillon, T. Akita, A. Grand, K. Kobayashi, E. Lelievre-Berna, J. Pecaut, E. Ressouche, J. Schweizer, *J. Am. Chem. Soc.* **1999**, *121*, 10126; b) Y. Pontillon, A. Caneschi, D. Gatteschi, A. Grand, E. Ressouche, R. Sessoli, J. Schweizer, *Chem. Eur. J.* **1999**, *12*, 3616; c) Y. Pontillon, E. Lelievre-Berna, A. Caneschi, D. Gatteschi, R. Sessoli, E. Ressouche, J. Schweizer, *J. Am. Chem. Soc.* **1999**, *121*, 5342; d) M. A. Aebersold, B. Gillon, O. Plantevin, L. Pardi, O. Kahn, P. Bergerat, I. von Seggern, F. Tuzek, L. Ohlstrom, A. Grand, E. Lelievre-Berna, *J. Am. Chem. Soc.* **1998**, *120*, 5238; e) E. Ressouche, J. X. Boucherle, B. Gillon, P. Rey, J. Schweizer, *J. Am. Chem. Soc.* **1993**, *115*, 3610.
- [11] For more details, see: B. Gillon, J. Schweizer in *The Interest in Polarized Neutron Diffraction. In Molecules in Physics, Chemistry, and Biology, Vol. II* (Ed: Jean Maruani), Kluwer Academic Publisher, Dordrecht, **1989**, p. 111.
- [12] The refinement was done using a modification of the least-squares refinement program MOLLY: N. K. Hansen, P. Coppens, *Acta Crystallogr. A* **1978**, *34*, 909.
- [13] A model-free spin density reconstruction (the Maximum of Entropy method; see ref. [10]) has also been performed. The corresponding map shows that the main part of the spin density is carried by the two C-C-N-C-C fragments and on the Ti atom, as obtained in the refinement.
- [14] *Amsterdam Density Functional (ADF) Scientific Computing and Modelling, Revision 02 1999*, Vrije Universiteit Amsterdam.
- [15] R. S. Mulliken, *J. Chem. Phys.* **1955**, *23*, 1833.
- [16] a) J. C. Slater, *Quantum Theory of Molecules and Solids. Vol. 4: Self-Consistent Field for Molecules and Solids*, McGraw-Hill, New York, **1974**; b) S. H. Vosko, L. Wilk, M. Nusair, *Can. J. Phys.* **1980**, *58*, 1200; c) H. Stoll, C. M. E. Pavlidou, H. Preuss, *Theor. Chim. Acta* **1978**, *49*, 143.
- [17] a) C. Lee, W. Yang, R. G. Parr, *Phys. Rev. B* **1988**, *37*, 785; b) A. D. Becke, *Phys. Rev. A* **1988**, *38*, 3098.

## A Novel Solid-Phase Assembly for Identifying Potent and Selective RNA Ligands\*\*

Nathan W. Luedtke and Yitzhak Tor\*


Replication of the human immunodeficiency virus (HIV-1) requires an ordered pattern of viral gene expression.<sup>[1]</sup> This process is dependent upon the association of Rev, an essential viral regulatory protein, with its respective RNA binding site, the Rev-response-element (RRE).<sup>[2]</sup> The RRE is necessary for the active export of unspliced genomic viral RNA from the nucleus and serves as part of the envelope–protein coding sequence.<sup>[2]</sup> This dual function makes the Rev–RRE binding event an attractive target for therapeutic intervention because the evolution of resistant variants may be prevented or impeded. Small molecules that specifically bind the RRE and preclude or competitively displace the Rev protein are therefore promising antiviral candidates.<sup>[3–5]</sup>

Aminoglycoside antibiotics have been shown to competitively block the binding of the Rev protein to the RRE, thus providing an important precedent for the use of low molecular weight ligands to target viral RNA sites.<sup>[3, 6]</sup> These natural antibiotics, however, bind the RRE with relatively low affinity and specificity.<sup>[7]</sup> Since aminoglycosides and most other RNA ligands appear to recognize certain RNA folds, rather than specific RNA sequences, the design and discovery of RNA ligands is a challenging and empirical process.<sup>[7b]</sup> Commonly employed RNA-binding assays are limited in their ability to probe both the affinity and specificity of potential binders.<sup>[7a, 8, 9]</sup> New approaches that allow the rapid determination of both the RNA affinity and specificity of small molecules will assist in the discovery of new lead compounds and advance the understanding of RNA recognition. To this end, we report the assembly of an immobilized RNA–protein complex and demonstrate its application to the discovery and characterization of new RNA binders.

The high-affinity Rev binding site within the RRE is the purine-rich bulge shown in Figure 1.<sup>[10]</sup> The arginine-rich segment, Rev<sub>34–50</sub>, binds the RRE with a dissociation constant similar to that of the full-length Rev protein.<sup>[11]</sup> We have developed an assay based on the competition between potential RNA binders and a fluorescent Rev peptide (“Rev-Fl”) for binding to an immobilized RRE fragment. The assay identifies small molecules that specifically interfere with Rev–RRE binding (Figure 1). Ligands that bind to the

[\*] Prof. Dr. Y. Tor, N. W. Luedtke  
Department of Chemistry and Biochemistry  
University of California, San Diego  
La Jolla, CA 92093-0358 (USA)  
Fax: (+1) 858-534-5383  
E-mail: ytor@ucsd.edu

[\*\*] We thank Professors David Wilson and David Boykin for a generous gift of the aromatic amidine derivatives and Professor Kol for a generous gift of eilatin-containing complexes. We are grateful to Dr. Georg Schlechtingen and Professor Murray Goodman for assistance with peptide synthesis and to Ibis Therapeutics for partial support. N.W.L. is supported by a National Institute of Health Molecular Biophysics Training Grant (GM 08326).

 Supporting information for this article is available on the WWW under <http://www.wiley-vch.de/home/angewandte/> or from the author.